



Multiple sulfur isotope systematics of Icelandic geothermal fluids and the source and reactions of sulfur in volcanic geothermal systems at divergent plate boundaries

Andri Stefánsson^{a,*}, Nicole S. Keller^a, Jóhann Gunnarsson Robin^a, Shuhei Ono^b

^a Institute of Earth Sciences, University of Iceland, Sturlugata 7, 101 Reykjavík, Iceland

^b Department of Earth, Atmospheric and Planetary Sciences, Massachusetts Institute of Technology, Cambridge, MA 02139, United States

Received 2 February 2015; accepted in revised form 28 May 2015; available online 6 June 2015

Abstract

Multiple sulfur isotope systematics of geothermal fluids at Krafla, Northeast Iceland, were studied in order to determine the source and reactions of sulfur in this system, as an example of a geothermal system hosted on a divergent plate boundary. Fluid temperatures ranged from 192 to 437 °C, and the fluids have low Cl concentration between ~10 and ~150 ppm, with liquid water and vapor being present in the reservoir. Dissolved sulfide (S^{-II}) and sulfate (S^{VI}) predominated in the water phase with trace concentrations of thiosulfate (S₂O₃²⁻) whereas sulfide (S^{-II}) was the only species observed in the vapor phase. The reconstructed sulfur isotope ratios of the reservoir fluids based on samples collected at surface from two-phase and vapor only well discharges indicated that $\delta^{34}\text{S}$ and $\Delta^{33}\text{S}$ of sulfide in the reservoir fluid ranged from -1.5 to +1.1‰ and -0.001 to -0.017‰, respectively, whereas $\delta^{34}\text{S}$ and $\Delta^{33}\text{S}$ of sulfate were significantly different and ranged from +3.4 to +13.4‰ and 0.000 to -0.036‰, respectively. Depressurization boiling upon fluid ascent coupled with progressive fluid–rock interaction and sulfide mineral (pyrite) formation results in the liquid phase becoming progressively isotopically lighter with respect to both $\delta^{34}\text{S}$ and $\Delta^{33}\text{S}$. In contrast, H₂S in the vapor phase and pyrite become isotopically heavier. The observed $\Delta^{33}\text{S}$ and $\delta^{34}\text{S}$ systematics for geothermal fluids at Krafla suggest that the source of sulfide in the reservoir fluids is the basaltic magma, either through degassing or upon dissolution of unaltered basalts. At high temperatures, insignificant SO₄ was observed in the fluids but below ~230 °C significant concentrations of SO₄ were observed, the source inferred to be H₂S oxidation. The two key factors controlling the multiple sulfur isotope systematics of geothermal fluids are: (1) the isotopic composition of the source material and (2) the isotope fractionation associated with aqueous and vapor speciation and how these change as a function of processes occurring in the system, including boiling, oxidation and fluid–rock interaction.

© 2015 Elsevier Ltd. All rights reserved.

1. INTRODUCTION

Sulfur is among the major components in volcanic geothermal fluids and is found both in the liquid and the vapor phase. Dissolved sulfide (S^{-II}) and sulfate (S^{VI}) predominate in the liquid phase whereas sulfide (S^{-II}) is the

predominant form in the vapor phase (e.g. Giggenschbach, 1980; Arnórsson et al., 1983a,b; Marini et al., 2011). Less abundant sulfur species have been observed including thio-sulfate (S₂O₃²⁻), sulfite (SO₃²⁻), polythionates (S_nO₆²⁻) and polysulfides (S_n²⁻) (Xu et al., 1998, 2000; Druschel et al., 2003; Kamyshny et al., 2008; Kaasalainen and Stefánsson, 2011a,b). The sulfur compounds in geothermal fluids may originate from various sources including meteoric water or seawater leaching from the host rock (altered

* Corresponding author. Tel.: +354 5254252.
E-mail address: as@hi.is (A. Stefánsson).

or fresh) or magmatic degassing. In seawater and meteoric water sulfur is predominantly present as sulfate, whereas sulfate and sulfide may be both present in the host rock depending on the formation conditions, i.e. sulfur dioxide and hydrogen sulfide are the stable forms of sulfur in magmatic gas, depending on temperature (Marini et al., 2011, and references therein).

The sources and reactions of sulfur compounds in volcanic geothermal fluids have been mainly approached using $\delta^{34}\text{S}$ systematics and equilibrium thermodynamics for fluid species and fluid–rock interaction. It is generally accepted that the concentrations of most major components are controlled by near equilibrium between the fluids and the secondary minerals within the reservoir (Giggenbach, 1980, 1981; Arnórsson et al., 1983a,b). However, for redox sensitive compounds like sulfur this may not be the case (e.g. Stefánsson and Arnórsson, 2002; Kaasalainen and Stefánsson, 2011b). Sulfur isotope exchange between sulfate and sulfide becomes sluggish below $\sim 250\text{ }^\circ\text{C}$; thus these two species may indicate isotope disequilibrium to temperatures as high as $200\text{--}300\text{ }^\circ\text{C}$ (e.g. Ohmoto and Lasaga, 1982).

Sparse data exist for $\delta^{34}\text{S}$ ratios of volcanic geothermal fluids and almost none are available for multiple sulfur isotope ratios. Based on available data, $\delta^{34}\text{S}$ values for sulfide in the water and vapor phase range from -4.4 to $+7.9\text{‰}$, whereas $\delta^{34}\text{S}$ values for dissolved sulfate range from -2.0 to $+23.1\text{‰}$ (Fig. 1) (Sakai et al., 1980; Sakai, 1983; Torssander, 1986; Robinson, 1987; Giggenbach, 1992; Matsuda et al., 2005; Bayon and Ferrer, 2005; González-Partida et al., 2005). For fluids at convergent plate boundaries, the sulfate is enriched in ^{34}S and can approach that of seawater, whereas the few values at divergent plate boundaries are similar to the sulfide ratios. Based on these findings it has been concluded that in most cases, the sources of sulfide and sulfate dissolved in geothermal fluids are likely to be the mantle and seawater, and the variations in sulfur isotope ratios are related to various processes including reduction of sulfate, oxidation of sulfide, formation of secondary sulfides and sulfates, and

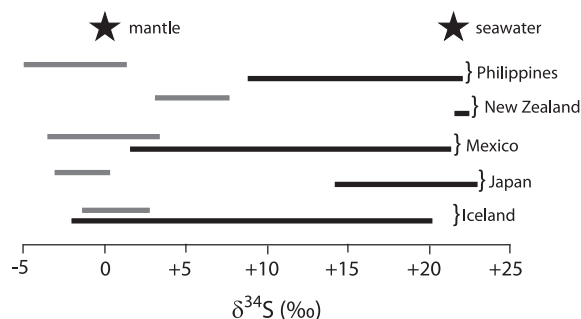


Fig. 1. Distribution of $\delta^{34}\text{S}$ ratios in geothermal fluids (water and vapor) from various locations in the world. Based on literature values reported by Sakai et al. (1980), Sakai (1983), Robinson (1987), Giggenbach (1992), Matsuda et al. (2005), Bayon and Ferrer (2005), González-Partida et al. (2005) and Marini et al. (2011) together with the values obtained in this study. The black lines indicate SO_4 whereas the gray lines indicate sulfide (in water or vapor).

disproportionation of magmatic SO_2 forming H_2S and SO_4 (e.g. Sakai et al., 1980; Bayon and Ferrer, 2005; Marini et al., 2011). However, there are further processes that may play an important role in affecting sulfur isotope ratios in geothermal fluids, namely fluid phase relation changes such as boiling which, among other things, affects the aqueous speciation of sulfur species as well as progressive fluid–rock interaction and secondary mineral formation.

Multiple sulfur isotope systematics provide a useful tool to trace a wide range of processes, including not only boiling and progressive fluid–rock interaction, but also oxidation and reduction of various sulfur species and fluid mixing and how speciation of sulfur compounds changes within the volcanic system as a consequence of these processes. The purpose of this study was to investigate the multiple sulfur isotope systematics in volcanic geothermal fluids fed by meteoric water on a divergent plate boundary, exemplified by the Krafla geothermal system in Northeastern Iceland. For this purpose, vapor and liquid samples were collected from two-phase well discharges and analyzed for sulfur isotope ratios of sulfide in the vapor phase and sulfide and sulfate in the liquid phase. Using geochemical modelling, the sulfur isotopic composition of the reservoir was assessed as well as sulfur isotope systematics upon water–vapor (boiling) and fluid–rock interaction. In this way, the source and reactions of sulfur in the geothermal fluids were traced.

2. METHODS

2.1. Sampling and analysis of major elements

Samples of two-phase geothermal well discharges at the Krafla geothermal field in Northeast Iceland were collected and analyzed for major elemental composition and multiple sulfur isotope ratios.

The liquid and vapor phase were separated at the well-head using a Webre separator. Vapor samples were collected into evacuated gas bulbs containing $5\text{--}10\text{ ml}$ 50% w/v KOH. The concentrations of CO_2 and H_2S in the vapor condensate were determined by modified alkalinity titration (Stefánsson et al., 2007) and a precipitation titration method using Hg-acetate and dithizone indicator (Arnórsson et al., 2006), respectively. The non-condensable gases including H_2 , N_2 , Ar and CH_4 were analyzed by gas chromatography (PerkinElmer-ARNEL 4019 Analyzer).

The liquid phase samples were cooled down using a stainless steel spiral separator connected to the Webre separator and then filtered through a $0.2\text{ }\mu\text{m}$ cellulose acetate filter into polypropylene (for major anion and cation analyses) and amber glass bottles (for CO_2 analyses). Samples for major cation analysis were acidified with 0.5 ml concentrated HNO_3 (Suprapur[®], Merck) per 100 ml sample and determined using ICP-OES (Spectro Ceros Vision). Two samples for major anion analysis were collected, one untreated and used for F, Cl and S_2O_3 determination and another to which 2% Zn-acetate solution was added to precipitate dissolved sulfide as zinc sulfide leaving dissolved SO_4 in solution for analysis. All anion analyses were carried

out using ion chromatography (Dionex ICS-2000). The IC analyses were carried out on the same day as sampling to minimize changes in sulfur speciation, particularly oxidation of S_2O_3 . Samples for determination of CO_2 were collected into amber glass bottles and analyzed using the modified alkalinity titration previously mentioned (Stefánsson et al., 2007). Dissolved sulfide ($\Sigma S^{II} = HS^-$ and $H_2S(aq)$) were titrated on-site using the method previously described (Arnórsson et al., 2006). The pH was analyzed on-site and in-line within a few seconds of sampling at $\sim 20^\circ C$ using a flow-through pH cell.

2.2. Sampling and analysis of multiple sulfur isotopes

As for the samples for major elements, samples of water and vapor for sulfur isotope analysis were collected using a Webre separator. Liquid samples were filtered through $0.2\ \mu m$ cellulose acetate filters into 1 L polypropylene bottles to which 10 mL 1 M Zn-acetate solution were added to precipitate dissolved sulfide as ZnS. Vapor samples were collected into evacuated gas-bulbs containing 10–15 mL 50% w/v KOH and 10 mL 1 M Zn-acetate solution to precipitate H_2S as ZnS. The ZnS precipitate for both liquid and vapor samples were filtered through a $0.2\ \mu m$ filter and the solids collected from the filter paper. The filtered solution from the water phase sample was also collected, to which 5 mL 1 M $BaCl_2$ solution and 1 mL 1 M HCl was added in order to precipitate SO_4 as $BaSO_4$. The solid $BaSO_4$ was subsequently filtered off using a $0.2\ \mu m$ filter and the solids collected from the filter paper.

Extraction and purification of sulfide and sulfate samples were carried out in the following way. The ZnS solids were dissolved in 6 N HCl under N_2 atmosphere and the evolved H_2S gas was precipitated, first as ZnS in 50 ml of Zn-acetate solution, and then as Ag_2S by adding 5 ml 0.1 M $AgNO_3$ to the solution. The Ag_2S was then cleaned in deionized water and dried at $80^\circ C$ (Alt and Shanks, 1998, with modifications). To obtain the sulfur isotope composition of sulfate, the $BaSO_4$ precipitate was dried and reduced to H_2S under N_2 atmosphere using the Thode reagent (a mixture of H_3PO_2 , HCl and HI, described in Thode et al., 1961). The H_2S produced was precipitated as Ag_2S using the previously mentioned method, cleaned in deionized water and dried at $80^\circ C$.

Sulfur isotope ratios were analyzed according to the method described by Ono et al. (2006, 2012). Approximately 2 mg of Ag_2S powder were reacted with fluorine gas at $300^\circ C$ for >6 h to produce SF_6 . The SF_6 was then purified by a gas chromatography system equipped with two columns, mole sieve $5\ \text{Å}$ and HayesepQ, followed by analyses by a Thermoelectron MAT 253 isotope ratio mass spectrometer. Replicate analysis ($n = 28$) of IAEA-S-1 reference material yield a standard deviation of 2σ 0.26‰ , 0.014‰ and 0.19‰ for $\delta^{34}S$, $\Delta^{33}S$ and $\Delta^{36}S$ (Ono et al., 2012).

Sulfur isotope ratios are reported relative to an international reference material, using the standard notation

$$\delta^x S = \frac{(xS/^{32}S)_{\text{sample}}}{(xS/^{32}S)_{\text{VCDT}}} - 1 \quad (1)$$

where $x = 33, 34$ and 36 and VCDT is the Vienna-Cañon Diablo Troilite reference material. Note that the factor of 1000, often used in calculating relative isotope ratios, has been omitted (see Coplen, 2011, for a detailed discussion on this matter).

The multiple sulfur isotope ratios defined as $\Delta^x S$ are defined by,

$$\Delta^{33}S = \ln(\delta^{33}S + 1) - {}^{33}\theta \ln(\delta^{34}S + 1) \quad (2)$$

Additionally, one can define

$$\Delta^{36}S = \ln(\delta^{36}S + 1) - {}^{36}\theta \ln(\delta^{34}S + 1) \quad (3)$$

However, as pointed out by Ono et al. (2006) the accuracy of the $\delta^{36}S$ measurements do not allow deriving additional information on sulfur isotope systematics beyond that of $\delta^{33}S$. The results for $\delta^{36}S$ are reported in this study but not further discussed for this reason. The values for ${}^{33}\theta$ and ${}^{36}\theta$ used in this study were 0.515 and 1.90, respectively, if not otherwise indicated.

3. RESULTS

The fluids sampled at Krafla were dilute (14–235 ppm Cl) and consisted of both liquid water and vapor (Table 1). The concentrations of SO_4 and total dissolved sulfide (ΣS^{II}) in the water phase of the well discharges were found to range from 5–525 ppm to 25–121 ppm, respectively, and S_2O_3 was also observed, with concentrations in the range 0.3 to 39 ppm. Other sulfur compounds were not detected in the liquid phase (detection limit < 0.1 ppm). In the vapor phase H_2S was the only observed sulfur compound with concentrations between 44 and 1831 ppm. The sampling temperatures were between 138 and $437^\circ C$.

In the water phase, the $\delta^{34}S$ values for ΣS^{II} and SO_4 ranged from -0.2 to -1.8 and $+3.4$ to $+13.4\text{‰}$, respectively. The $\delta^{34}S$ values for H_2S in the vapor phase ranged from $+0.1$ to $+1.3\text{‰}$. The $\Delta^{33}S$ values for ΣS^{II} in the water phase were found to be between -0.001 and -0.019‰ , for SO_4 in the water phase between -0.004 and -0.036‰ and H_2S in the vapor phase between -0.000 and -0.012‰ .

4. DISCUSSION

4.1. $\delta^{34}S$ systematics in Icelandic rocks and fluids

The distribution of $\delta^{34}S$ values in geothermal water and vapor, pyrite, sulfates, as well as altered and unaltered bulk rock in Iceland is shown in Fig. 2. The data shown are those obtained in this study and previously reported by Sakai et al. (1980) and Torssander (1986, 1989). Unaltered basalt range from -2.0 to $+4.2\text{‰}$. Similar ratios were observed for ΣS^{II} and H_2S in geothermal water and vapor and pyrite for dilute geothermal systems (0 to $+2.6\text{‰}$). On the other hand, pyrite for geothermal systems with seawater as the source fluid, as at Reykjanes and Svartsengi, have more positive $\delta^{34}S$ values (-1.5 to $+7.9\text{‰}$) suggesting an influence from seawater sulfate. Moreover, in the saline geothermal systems in Iceland, SO_4 in the water, rock and sulfate minerals have $\delta^{34}S$ values between $+18.5$ to $+20.4\text{‰}$, close to seawater value (21.0‰ , Rees et al., 1978). In dilute

Table 1

Sulfur species concentration and sulfur isotope ratios in geothermal well discharges, Krafla NE Iceland. Concentrations are in ppm and isotope ratios in ‰.

Sample #	Well #	t^{sample} °C	$t^{\text{reservoir}}^{\text{a}}$ °C	h kJ/ kg	Liquid phase												Vapor phase					
					pH	/ °C	Cl	SO ₄	ΣS ^{-II}	S ₂ O ₃	ΣS ^{-II}	SO ₄			H ₂ S ^b	Cl	H ₂ S					
												δ ³⁴ S	Δ ³³ S	Δ ³⁶ S				δ ³⁴ S	Δ ³³ S	Δ ³⁶ S		
11-KRA-01	K-17	208	274 ^a	2399	8.80	/	23	17.90	5.36	102	0.28	-1.25	-0.002	-0.064				821	<1.0	0.50	-0.014	0.063
11-KRA-02	K-16A	181	259 ^a	2660	7.35	/	24	137.7	10.8	72.0	4.82	-0.67	-0.001	-0.001				1326	<1.0	1.26	-0.004	0.029
11-KRA-03	K-37	189		2767														1202	1.0	1.28	-0.012	-0.022
11-KRA-04	K-32	177	247 ^a	1468	9.12	/	18	42.0	280	103	0.27	-1.11	-0.016	-0.150	4.66	-0.008	0.089	799	<1.0	1.04	0.000	0.037
11-KRA-05	K-33	173	262 ^a	2769	8.42	/	19	97.6	7.26	120	1.44	-1.06	-0.009	0.046				1551	<1.0	0.33	-0.009	0.015
11-KRA-06	K-20	181	306 ^a	2776	8.25	/	17	244	5.10	97.0	0.42	-1.53	-0.008	-0.136				1375	<1.0	0.05	-0.016	0.109
11-KRA-07	K-14	180	245	2627														329	<1.0	0.84	-0.011	-0.028
11-KRA-08	K-24	138	209 ^a	852	9.59	/	18	44.2	223	28.4	1.89	-1.19	-0.010	0.059	4.29	-0.018	-0.026	44	<1.0	1.20	-0.009	-0.019
11-KRA-09	K-13A	171	232 ^a	1553	9.08	/	15	38.5	262	68.6	3.41	-1.73	-0.009	0.054	4.38	-0.016	0.026	625	<1.0	0.55	-0.001	0.068
11-KRA-10	K-21	179	244 ^a	1058	8.90	/	21	134.7	54.7	42.0	1.28	-1.70	-0.012	0.144	6.11	-0.029	0.129	400	<1.0	0.78	-0.003	0.041
11-KRA-11	K-05	138	206 ^a	998	9.22	/	16	41.4	218	27.6	9.26	-1.83	-0.010	0.104	3.40	-0.004	0.051	176	<1.0	0.78	-0.004	0.073
11-KRA-12	K-27	185	235 ^a	1370	9.25	/	15	38.0	252	42.8	28.2	-0.97	-0.019	0.000	3.82	-0.015	0.063	233	<1.0	1.11	-0.005	0.017
11-KRA-16	K-40	183	246 ^a	2774	6.49	/	9	20.7	19.9	32.8	6.43	-0.23	-0.001	0.034	13.37	-0.036	0.167	1034	<1.0	0.64	-0.010	-0.044
11-KRA-17	K-34	207	250 ^a	2763	7.27	/	9	157	52.2	63.0	39.1	-0.51	-0.015	-0.043	9.78	-0.025	-0.020	1833	<1.0	1.06	-0.014	0.049
	IDDP-1	437	437	3200														668	79.6	1.13	-0.014	-0.099
	IDDP-1	437	437	3200														617	118	0.52	-0.001	0.020

^a Reservoir temperature calculated using the quartz geothermometer (Gunnarsson and Arnórsson, 2000). The values reported are the average calculated values using the three models for reconstructed reservoir fluid composition (see text). In the case of dry steam discharge the sampling temperatures are just reported.

^b Concentrations are in mg H₂S per kg condensate that is >99% H₂O in all cases.

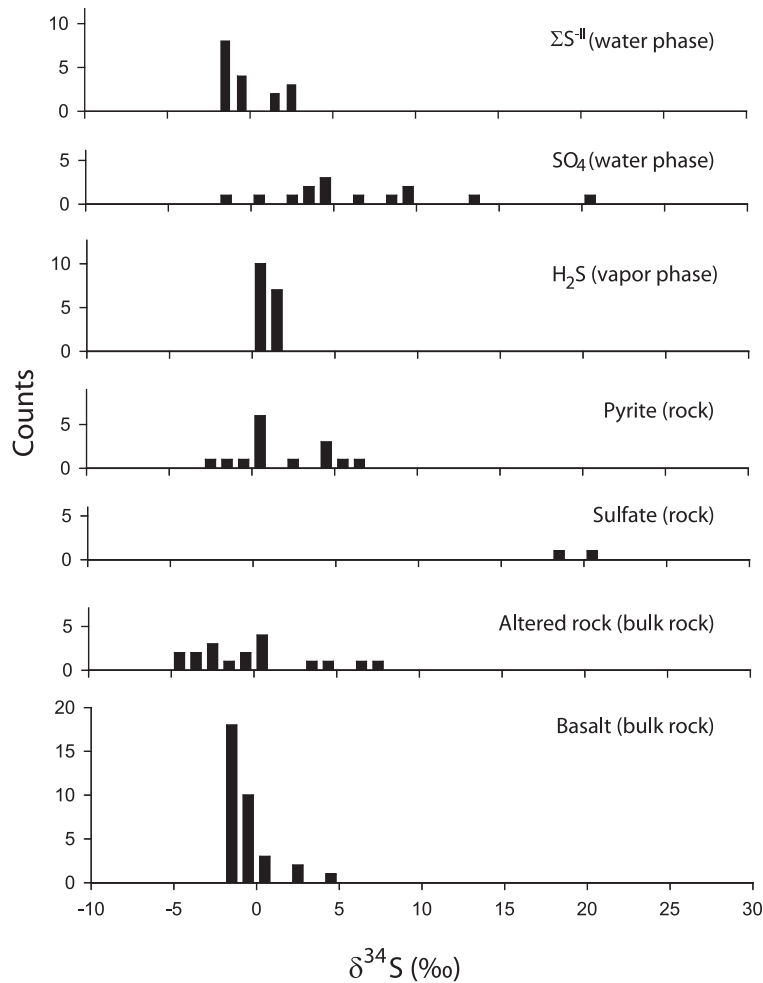


Fig. 2. Distribution of $\delta^{34}\text{S}$ in geothermal water, vapor, geothermally altered rocks and fresh basalts in Iceland. The results presented were those obtained in this study (Table 1) as well as those previously reported by Sakai et al. (1980) and Torssander (1986, 1989) for minerals, rocks and fluids.

geothermal systems, sulfate minerals are absent and the $\delta^{34}\text{S}$ range for aqueous SO_4 is between +3.4 and +13.4‰, much closer to rock and sulfide values than to seawater values.

4.2. Reservoir fluid composition and sulfur speciation

The assessment of sulfur chemistry and isotope systematics in the reservoirs of volcanic geothermal systems relies on the reconstruction of reservoir fluid compositions using the compositional data of the liquid and vapor discharge sampled at the surface from wells drilled into the reservoir. The reservoirs may be sub-boiling and only consist of a single liquid phase, consist of two phases (liquid and vapor) or consist of a single vapor phase (Fig. 3). For liquid only sub-boiling reservoirs, depressurization boiling occurs within the well. In this case it is reasonable to assume the system to be isolated. The water to vapor ratio of such well discharges is measured by the well enthalpy (h) and is typically <1200 kJ/kg. In the case of two-phase liquid and vapor and vapor only geothermal reservoirs, intensive

boiling occurs within the reservoir. Boiling may be caused by a pressure drop within the reservoir and/or by addition of heat, for example from a magma body. The measured vapor to liquid ratio of the well discharges at surface of such two-phase liquid and vapor and vapor only geothermal reservoirs is generally greater than that determined in single phase liquid reservoirs, with well discharge enthalpy typically 1200–2700 kJ/kg. Depressurization boiling leads to a temperature decrease of the fluid along the two-phase curve of water, whereas boiling due to addition of heat by conduction leads to constant temperature until pure vapor is formed (Henley and Hughes, 2000). Consideration of the physical properties of liquid water and vapor, fluid flow and chemical variability of well discharges as a function of vapor to liquid ratio suggest that depressurization boiling within the reservoir may lead to phase segregation (e.g. Arnórsson et al., 2007; Scott et al., 2014). In this case, the liquid phase is retained on mineral grain surfaces and the lower density vapor preferentially flows towards the well. The strong decrease in the relative permeability of liquid at intermediate vapor saturation and high capillary

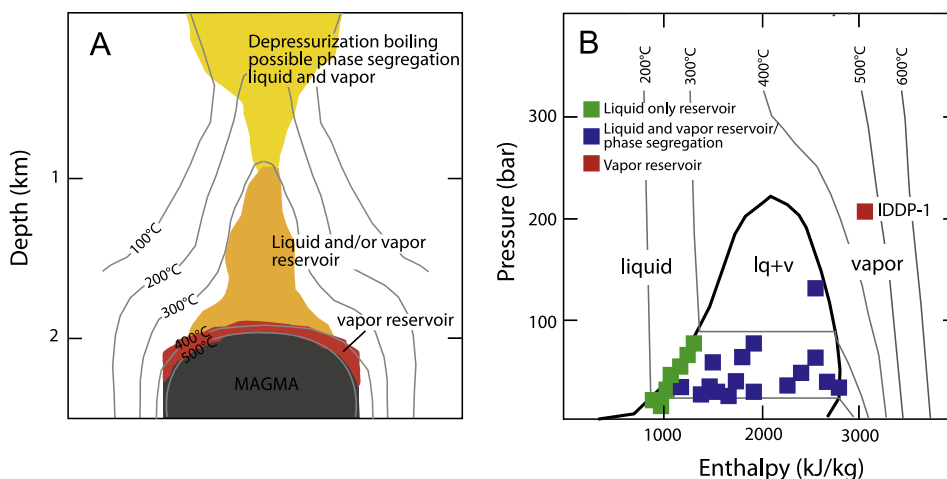


Fig. 3. (A) The simulated phase relations and temperature distribution of a ~ 2000 – 4000 year old geothermal system initially with a magmatic heat source with the top at 2 km depth, of basalt composition and having temperatures of 1100 °C. The simulations were carried out with the aid of the HYDROTHERM (Hayba and Ingebritsen, 1994) program with rock density of 2900 kg/m³, thermal conductivity 2 W/m K, rock compressibility of $1 \cdot 10^{-10}$ bar⁻¹, rock heat capacity, specific heat of 1 kJ/kg K at 0 – 750 °C to 2 kJ/kg K at 800 – 1200 °C and temperature dependent permeability of $1 \cdot 10^{-15}$ m² at 0 – 360 °C followed by a log dependent decrease from $1 \cdot 10^{-15}$ m² at 360 to $1 \cdot 10^{-22}$ m² at 500 °C taken to be the brittle-ductile boundary of the magmatic-geothermal system. At depth close to the basalt intrusion, the temperature was >400 °C and a single phase vapor (superheated or supercritical depending on pressure) was found, whereas at shallower depths, a single phase liquid or two-phase liquid+vapor reservoir was found depending on the age of the system. Upon fluid ascent, depressurization boiling occurred forming liquid and vapor with boiling as an isolated or open system process, the latter often referred to as phase segregation. The two-phase liquid and vapor reservoirs or open system boiling (phase segregation) resulted in excess vapor over water of the geothermal surface well discharges relative to a single phase liquid reservoir and measured reservoir temperatures, this phenomenon referred to as excess enthalpy character. (B) The measured phase relations in the Krafla geothermal system expressed as Enthalpy (h) – Pressure (P) diagram for water with temperature contours. The fluid–vapor phase relations observed at Krafla were similar to those calculated by the modelled young geothermal system with a magma heat source forming a single phase vapor at depth. Decrease in pressure (adiabatic rise of the fluid) can result in a single liquid phase reservoirs with $h < 1200$ kJ/kg, a two phase liquid and vapor reservoir or a reservoir with excess enthalpy with $h = 1200$ – 2700 kJ/kg formed either by reservoir boiling or induced by magmatic heat or phase segregation within the upflow zone of the geothermal system.

pressure contribute to causing liquid to adhere to mineral grain surfaces and remain in the reservoir (Sorey et al., 1980; Horne et al., 2000; Pritchett, 2005; Li and Horne, 2007). High vapor to liquid ratio of well discharges is an occurrence commonly referred to as “excess discharge enthalpy”. Excess enthalpy can be linked to two processes, namely conductive heat addition and vapor–liquid phase segregation. These processes results in very different concentration patterns of non-volatiles in the fluid discharge with increasing discharge enthalpy, as shown in Fig. 4 using SiO₂ compositions as an example of a non-volatile element. Conductive heat addition leads to increased concentrations of non-volatiles in the liquid phase, whereas the concentration in the total discharge remains constant with increasing enthalpy. On the other hand, vapor–liquid phase segregation leads to a constant concentration of non-volatiles in the liquid phase whereas the concentration in the total discharge decreases with increasing enthalpy.

Many of the well discharges at Krafla showed excess enthalpy, the cause being phase segregation or conductive heat addition or a combination of both processes (Fig. 4). Because it is not known which of these processes is at play in the geothermal system, three different models were used to calculate the reservoir fluid compositions from two-phase well discharge data: (1) assuming no vapor in the reservoir, (2) assuming that the excess enthalpy was the consequence of heat addition, and (3) assuming that

the excess enthalpy of the well discharges was the consequence of phase segregation. These three models are referred to as the isolated system boiling model (no vapor in the reservoir), the conductive heat model (excess enthalpy caused by heat addition) and the phase segregation model (excess enthalpy caused by depressurization boiling followed by phase segregation). The calculations were carried out using the WATCH program (Bjarnason, 2010) and are based on formulations derived and given by Arnórsson et al. (2007). Three sets of parameters are needed in order to calculate the reservoir fluid composition from the wellhead data: (1) the measured temperature and vapor to liquid ratio (enthalpy) of the well discharge, (2) the temperature and vapor to liquid ratio of the reservoir, and (3) the temperature or pressure where phase segregation occurred. For the present study the reservoir temperature was based on the quartz geothermometer (Gunnarsson and Arnórsson, 2000). Selection of the phase segregation temperature or pressure is less straightforward, as phase segregation likely occurs over a temperature or pressure interval rather than at a single point. Following Arnórsson et al. (2007) the segregation temperature was assumed to be approximately halfway between the initial reservoir fluid temperature and the wellhead temperature.

It is generally accepted that the concentrations of major elements in geothermal fluids, except for incompatible elements like Cl, are controlled by near equilibrium with

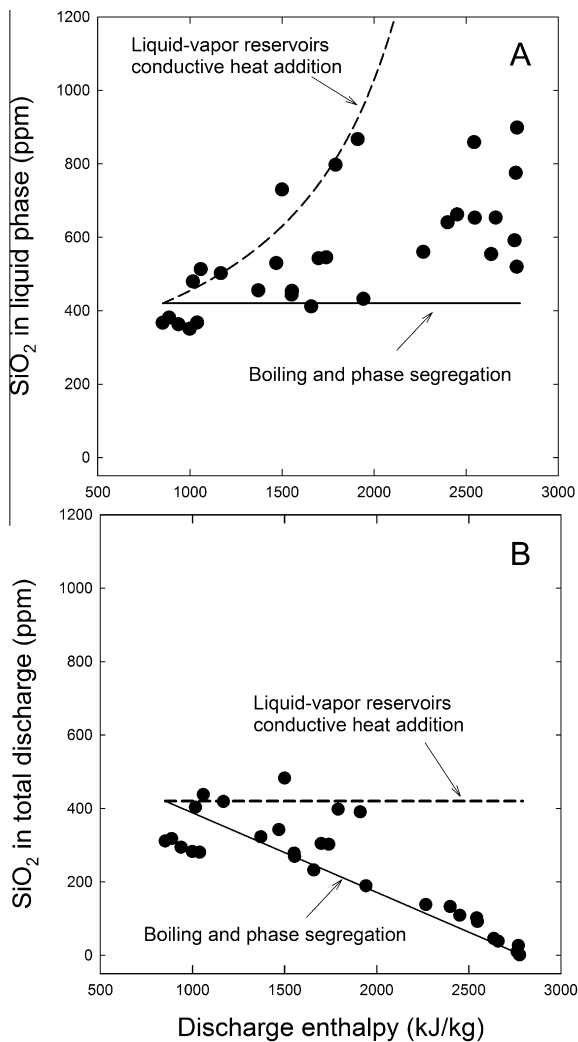
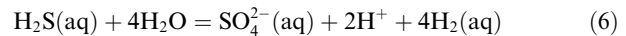
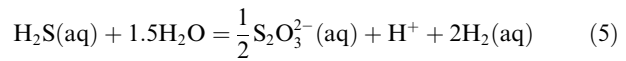
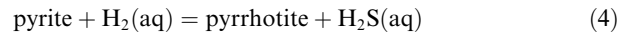


Fig. 4. The concentration of SiO₂ in the liquid phase (A) and total two-phase discharge (B) as a function of measured vapor to liquid ratio of the well fluids discharge at surface, expressed as discharge enthalpy. In (A), dots represent measured SiO₂ concentrations in the liquid samples at the wellhead, whereas in (B) the dots represent the recalculated SiO₂ concentrations in the total discharge, taking the steam fraction into account. In both graphs, the black dashed and solid lines represent heat addition and phase segregation model lines of SiO₂ concentration as a function of discharge enthalpy. The effects of conductive heat addition and phase segregation were calculated at a constant temperature of 200 °C for fluids having an initial SiO₂ concentration of 420 ppm. The calculations were carried out with the aid of the WATCH program. As observed, two processes were likely to be the cause of excess discharge well enthalpy (too high vapor to liquid ratio relative to the reservoir temperature and assuming liquid only reservoir). Firstly, the excess vapor may have been the result of conductive heat in the reservoir, for example from a magma body, causing reservoir vapor fraction. Alternatively, drilling may have resulted in pressure drawdown in the reservoir resulting in reservoir boiling and vapor and liquid separation. The data shown in the plot are those obtained in this study together with literature data (Gudmundsson and Arnórsson, 2005; Giroud, 2008).

secondary minerals observed in the geothermal systems (e.g. Gignenbach, 1980, 1981; Arnórsson et al., 1983a,b).

On the other hand, redox equilibria may not be attained between aqueous species and gases in the system H–O–S–C–N, even at temperatures as high as 300 °C (Stefánsson and Arnórsson, 2002). In addition, isotope fractionation among H₂S and SO₄ has been observed to be in isotope disequilibrium in geothermal fluids (Ohmoto and Lasaga, 1982). In order to assess chemical equilibrium among the common sulfide minerals and sulfur species at Krafla the following reactions were considered:



Pyrite and pyrrhotite have both been observed to occur within the Krafla geothermal system (Steinþórsson and Sveinbjörnsdóttir, 1981) and the only detected sulfur components in the fluids are ΣS^{-II}, SO₄ and S₂O₃ in water and H₂S in vapor are (Kaasalainen and Stefánsson, 2011b; this study).

The aqueous species activities were calculated with the aid of the WATCH program (Bjarnason, 2010) from the reservoir composition determined using the three models discussed above. Additional data on fluid composition reported by Gudmundsson and Arnórsson (2005) and Giroud (2008) were also included, together with the data reported in Table 1. The equilibrium constants for the respective reactions were calculated using the Supcrt92 program (Johnson et al., 1992) and the slop07.dat database (<http://geopig.asu.edu/sites/default/files/slop07.dat>). The equilibrium conditions were calculated at 200 and 300 °C at water vapor saturation pressure (P_{sat}) and 400 and 500 °C at 500 bar.

The results of chemical equilibrium calculations among sulfur bearing minerals and aqueous species largely depend on the approach used for calculating the reservoir composition (Fig. 5). The reservoir temperatures, calculated using the quartz geothermometers and reported as the average of the results from the three models, were determined to be in the range of 192–330 °C for most wells, with the IDDP-1 well having a higher temperature of 437 °C (Table 1). This was somewhat lower than the predicted equilibrium temperatures for the various sulfur bearing mineral and redox reactions. The causes for these discrepancies may be many. Firstly, problems related to sampling and chemical analysis could lead to inaccurate results. However, the sampling and analytical techniques used here are considered reliable (e.g. Arnórsson et al., 2006; Kaasalainen and Stefánsson, 2011a,b), and thus this source of error is considered unlikely. Secondly, the thermodynamic data, used both to calculate the aqueous speciation and to predict the reaction equilibrium constants, may be uncertain. For example, Pokrovski and Dubrovinsky (2011) suggested that S³⁻ may be a key species in hydrothermal fluids at >300 °C, yet this species is not included here. Thirdly, the data acquired from sampling of the surface discharge may not represent the aqueous speciation of sulfur compounds at the reservoir as reactions may occur within the well upon fluid ascent to the surface.

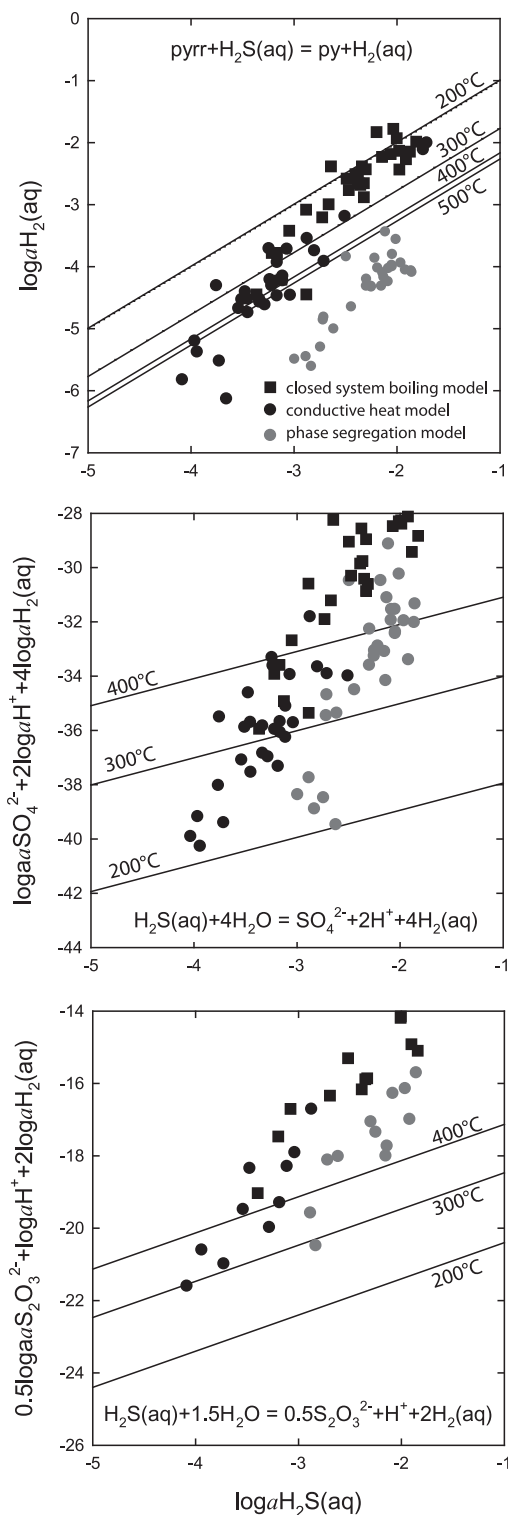


Fig. 5. Chemical equilibria among H_2S , S_2O_3 , and SO_4 and sulfur-bearing minerals, according to Eqs. (4)–(6) in the text. The dots and squares show the calculated activity products for given reactions and the lines show the calculated equilibrium concentrations at 200 and 300 °C water vapor saturation pressure, and 400 and 500 °C at 500 bar. The results of the three models used for calculation of the reservoir fluid composition based on fluid well discharge at surface are shown by the different symbols.

However, it should be kept in mind that the temperature change from reservoir to surface sampling is usually <100 °C. Based on these facts and following Stefánsson and Arnórsson (2002) it is difficult to assess if overall equilibrium exists among sulfur species and sulfur-bearing minerals under hydrothermal conditions in dilute fluids at <300 °C like those observed at Krafla.

4.3. Sulfur isotope systematics upon boiling and geothermal reservoir sulfur isotope ratios

In order to reconstruct the sulfur isotope ratios in the geothermal reservoir using well discharge data, the three models discussed previously were extended to include multiple sulfur isotope fractionation upon vapor–liquid interaction and associated aqueous species distribution changes. The calculations involved two steps: firstly, calculation of liquid and vapor distribution upon boiling and the associated aqueous and vapor speciation and, secondly, sulfur isotope distribution among the aqueous and vapor species. The species included in the calculations upon boiling were $\text{H}_2\text{S}(\text{g})$, $\text{H}_2\text{S}(\text{aq})$ and $\text{HS}^-(\text{aq})$. Aqueous SO_4 was not included as it does not partition between the water and vapor phase upon boiling and $\text{SO}_4^{2-}(\text{aq})$ was the dominant sulfate species under all conditions. It follows that the measured SO_4 isotope ratios of the surface discharge reflected those of the reservoir.

For the reconstruction of the reservoir fluid isotope ratios, the system was assumed to be isotopically closed upon boiling, and the following mass balance equation was used:

$$\delta^x \text{S}^{\text{total}} = X_{\text{H}_2\text{S}(\text{g})} \delta^x \text{S}_{\text{H}_2\text{S}(\text{g})} + X_{\text{H}_2\text{S}(\text{aq})} \delta^x \text{S}_{\text{H}_2\text{S}(\text{aq})} + X_{\text{HS}^-(\text{aq})} \delta^x \text{S}_{\text{HS}^-(\text{aq})} \quad (7)$$

where X_i are the appropriate mole fractions of $\text{H}_2\text{S}(\text{g})$, $\text{H}_2\text{S}(\text{aq})$ and $\text{HS}^-(\text{aq})$ and x stands for sulfur 33, 34 or 36. The fractionation factor α between two aqueous and/or vapor species i and j is defined by

$$x_\alpha = \frac{1000 + \delta^x S_i}{1000 + \delta^x S_j} \quad (8)$$

By combining the fractionation factors relative to $\text{H}_2\text{S}(\text{aq})$ (i.e. $j = \text{H}_2\text{S}(\text{aq})$ in Eq. (8)) and the mass balance equation (Eq. (7)) it follows that

$$\begin{aligned} \delta^x \text{S}^{\text{total}} = & X_{\text{H}_2\text{S}(\text{aq})} \delta^x \text{S}_{\text{H}_2\text{S}(\text{aq})} \\ & + X_{\text{H}_2\text{S}(\text{g})} ((^x \alpha_{\text{H}_2\text{S}(\text{g})-\text{H}_2\text{S}(\text{aq})} (1000 + \delta^x \text{S}_{\text{H}_2\text{S}(\text{aq})})) \\ & - 1000) + X_{\text{HS}^-} ((^x \alpha_{\text{HS}^--\text{H}_2\text{S}(\text{aq})} (1000 \\ & + \delta^x \text{S}_{\text{H}_2\text{S}(\text{aq})})) - 1000) \end{aligned} \quad (9)$$

where $\delta^x S_i$ is expressed per mil. Using the isotope fractionation factors, $\delta^x \text{S}^{\text{total}}$ and the mole fraction of the appropriated aqueous and vapor species, the isotope ratios for $\text{H}_2\text{S}(\text{g})$, $\text{H}_2\text{S}(\text{aq})$ and $\text{HS}^-(\text{aq})$ were calculated. The values for the fractionation factors used in these calculations are given in Table 2 and are based on values reported by Ohmoto and Rye (1979) for $\text{SO}_4/\text{H}_2\text{S}(\text{aq})$, Otake et al. (2008) for $\text{H}_2\text{S}(\text{aq})/\text{HS}^-(\text{aq})$ and Czarnacki and Halas (2012) for $\text{H}_2\text{S}(\text{aq})/\text{H}_2\text{S}(\text{g})$. Smoothed fractionation factors

Table 2
Temperature functions to calculate smoothed fractionation factors of sulfur 33, 34 and 36 isotope ratios. The functions are based on values reported by Ohmoto and Rye (1979), Otake et al. (2008) and Czarnacki and Halas (2012).

	$^{33}\alpha$			$^{34}\alpha$			$^{36}\alpha$		
	A	B	C	A	B	C	A	B	C
	$10^3 \ln \alpha = A + B/T + C/T^2$								
$\alpha_{H_2S(g)-H_2S(aq)} = \frac{1000 + \delta^{33}S_{H_2S(g)}}{1000 + \delta^{33}S_{H_2S(aq)}}$	0.0301147	44.495329	-63232.52	0.05847522	86.398698	-122781.59	0.1111029	164.15753	-233285.02
$\alpha_{HS^-(aq)-H_2S(aq)} = \frac{1000 + \delta^{33}S_{HS^-(aq)}}{1000 + \delta^{33}S_{H_2S(aq)}}$	0.5060551	-1008.9084	-44883.045	0.97597038	-1947.3864	-90069.458	1.8534845	-3682.8757	-165168.62
$\alpha_{SO_4^{2-}-H_2S(aq)} = \frac{1000 + \delta^{33}S_{SO_4^{2-}}}{1000 + \delta^{33}S_{H_2S(aq)}}$	-3.7999529	5268.1093	1753303.1	-7.34135139	10167.868	3421169.4	-13.784628	19056.652	6553556.5
$\alpha_{pyrite-H_2S(aq)} = \frac{1000 + \delta^{33}S_{pyrite}}{1000 + \delta^{33}S_{H_2S(aq)}}$	0	0	206,000	0	0	400,000	0	0	760,000

were obtained for the purpose of our study by fitting the reported values to a function of $10^3 \ln \alpha = A + B/T + C/T^2$ using least squares regression.

The effects of boiling upon multiple sulfur isotope fractionation between $H_2S(g)$, $H_2S(aq)$ and $HS^-(aq)$ are demonstrated in Figs. 6 and 7. Depressurization boiling along the water vapor saturation curve resulted in partitioning of volatile species like H_2S and CO_2 into the vapor phase. This resulted in a pH increase of the water phase and changed the relative abundances of $H_2S(aq)$ and $HS^-(aq)$ (Fig. 6). The $H_2S(g)$ and $H_2S(aq)$ species were isotopically similar, yet $H_2S(aq)$ became slightly heavier relative to $H_2S(g)$ upon progressive boiling (Fig. 7). Sulfur isotope fractionation between $H_2S(aq)$ and $HS^-(aq)$, however, was significant with $\delta^{34}S$ values of approximately -4 to -2.5‰ at 100–300 °C and $\Delta^{33}S$ ranging from -0.004 to 0.000‰. Overall, the combined changes in aqueous speciation and vapor formation associated with progressive boiling resulted in the liquid phase becoming isotopically lighter and the vapor phase becoming isotopically heavier.

Based on these findings, the multiple sulfur isotope ratios of reservoir sulfide (ΣS^{II}) were calculated based on the three boiling models described previously. The results are listed in Table 3 and shown in Fig. 8. The results were somewhat dependent on the model used, i.e. whether the excess discharge enthalpy is assumed to be caused by

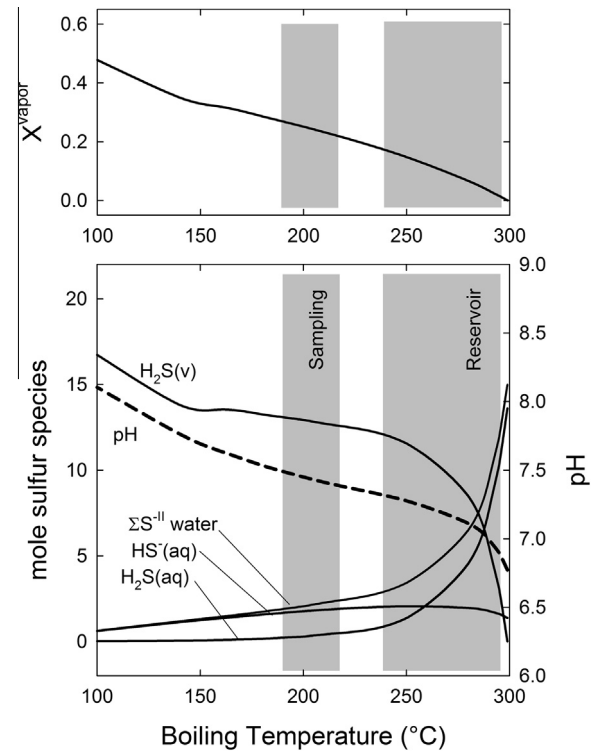


Fig. 6. The effects of closed system boiling on aqueous speciation of dissolved sulfide sulfur. Upon depressurization boiling $H_2S(aq)$ partitions into the vapor phase resulting in increased $H_2S(v)$ mole fraction and decreased dissolved sulfide in the liquid phase, i.e. $\Sigma S^{II} = H_2S(aq) + HS^-(aq)$. This, together with loss of CO_2 into the vapor phase, led to increased pH of the boiled water resulting in the ionization of $H_2S(aq)$ to HS^- . Also shown (gray shaded areas) are the range of reservoir and sampling temperatures at Krafla.

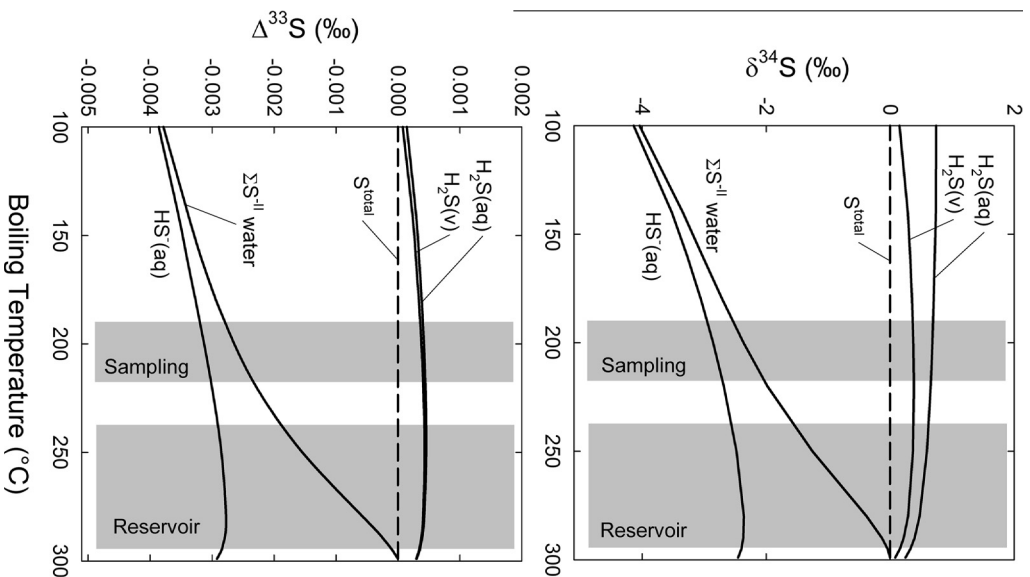


Fig. 7. The effects of closed system boiling on sulfur isotope ratios ($\delta^{34}\text{S}$ and $\Delta^{33}\text{S}$) of $\text{H}_2\text{S}(\text{v})$, $\text{H}_2\text{S}(\text{aq})$, $\text{HS}^-(\text{aq})$ and total dissolved sulfide in the water phase, i.e. $\Sigma\text{S}^{\text{II}} = \text{H}_2\text{S}(\text{aq}) + \text{HS}^-(\text{aq})$. Upon boiling, $\text{H}_2\text{S}(\text{aq})$ became isotopically heavier relative to $\text{H}_2\text{S}(\text{v})$, as one would expect. However, associated with the boiling and acid loss to the vapor phase, the solution pH increased and $\text{H}_2\text{S}(\text{aq})$ ionized to HS^- causing large sulfur isotope fractionations and leading to lighter sulfur isotope ratios in the liquid phase.

conductive heat addition or by depressurization boiling and phase segregation. Nevertheless, all the model calculations displayed a range of $\delta^{34}\text{S}$ ratios overlapping with that observed for unaltered Icelandic basalts, a fact pointing towards basalt as the source of sulfide sulfur in these systems (Fig. 8). In contrast, $\delta^{34}\text{S}$ values for SO_4 are much higher, in the range of +3.4 to +13.4‰.

4.4. Sulfur isotope systematics upon fluid–rock interaction and geothermal reservoir sulfur isotope ratios

Fluid–rock interaction is considered to exert a major effect on sulfur chemistry and isotope systematics in geothermal systems. In order to study possible variations in sulfur concentrations and sulfur isotope systematics associated with fluid–rock interaction, a geochemical model was

Table 3

Multiple sulfur isotope ratios in reservoir fluids calculated from the isotope composition of the discharge fluids and the appropriate model to reconstruct the reservoir fluids.

Sample #	Well #	Reservoir vapor phase						Total S^{II} reservoir (vapor + liquid)					
		SO_4			Closed boiling model			Conductive heat model			Phase segregation model		
		$\delta^{34}\text{S}$	$\Delta^{33}\text{S}$	$\Delta^{36}\text{S}$	$\delta^{34}\text{S}$	$\Delta^{33}\text{S}$	$\Delta^{36}\text{S}$	$\delta^{34}\text{S}$	$\Delta^{33}\text{S}$	$\Delta^{36}\text{S}$	$\delta^{34}\text{S}$	$\Delta^{33}\text{S}$	$\Delta^{36}\text{S}$
11-KRA-01	K-17				−1.0	−0.003	−0.045	0.1	−0.011	0.037	−0.7	−0.005	−0.027
11-KRA-02	K-16A				−0.3	−0.001	0.004	1.1	−0.004	0.027	−0.2	−0.002	0.006
11-KRA-03													
11-KRA-04	K-32	4.7	−0.008	6.539	−0.8	−0.014	−0.121	−0.3	−0.010	−0.084	−0.6	−0.012	−0.104
11-KRA-05	K-33				−0.7	−0.009	0.039				−0.7	−0.009	0.038
11-KRA-06	K-20				−1.1	−0.010	−0.070				−1.2	−0.009	−0.089
11-KRA-07					0.8	−0.011	−0.028						
11-KRA-08	K-24	4.3	−0.018	5.922				−0.8	−0.010	0.047	−0.6	−0.010	0.040
11-KRA-09	K-13A	4.4	−0.016	6.090	−1.4	−0.008	0.056	−0.8	−0.006	0.060	−1.2	−0.007	0.057
11-KRA-10	K-21	6.1	−0.029	8.589	−1.3	−0.011	0.129	−1.3	−0.011	0.128	−1.1	−0.010	0.119
11-KRA-11	K-05	3.4	−0.004	4.759	−1.5	−0.009	0.100	−1.3	−0.009	0.098	−1.3	−0.009	0.099
11-KRA-12	K-27	3.8	−0.015	5.347	−0.7	−0.017	0.002	−0.4	−0.015	0.005	−0.5	−0.016	0.004
11-KRA-16	K-40	13.4	−0.036	18.679	−0.1	−0.003	0.023	0.6	−0.010	−0.044	−0.2	−0.002	0.030
11-KRA-17	K-34	9.8	−0.025	13.523	−0.3	−0.015	−0.031	1.0	−0.014	0.048	−0.1	−0.014	−0.020
	IDDP-1				1.1	−0.014	−0.099	1.1	−0.014	−0.099	1.1	−0.014	−0.099
	IDDP-1				0.5	−0.001	0.020	0.5	−0.001	0.020	0.5	−0.001	0.020

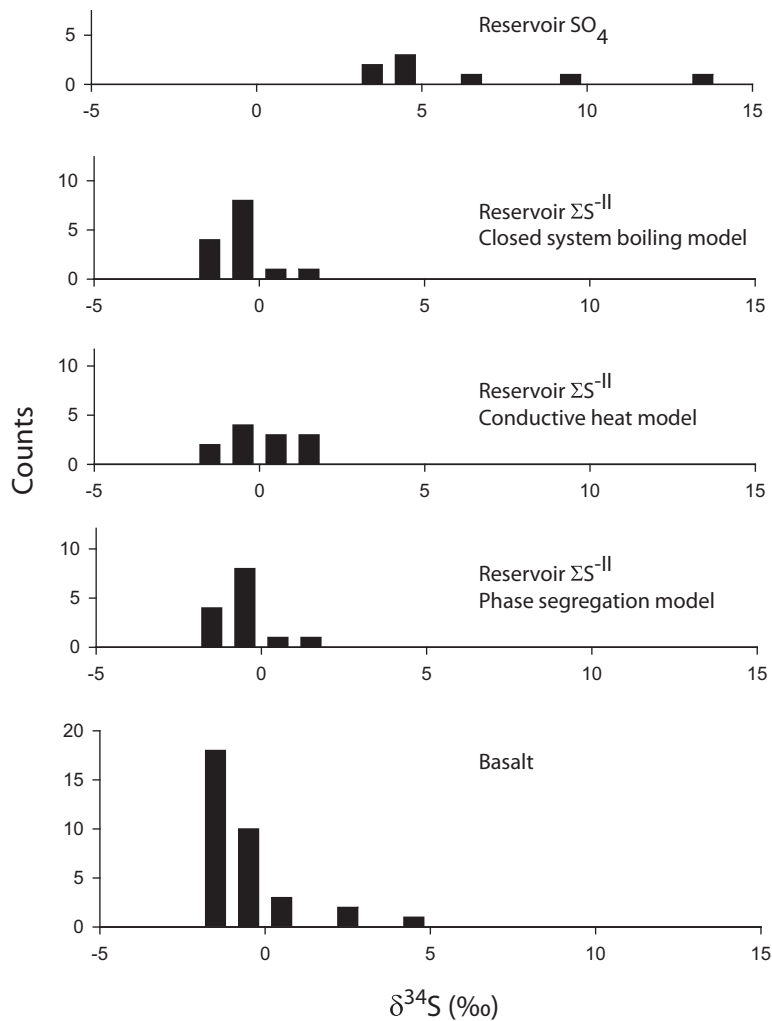


Fig. 8. The calculated $\delta^{34}\text{S}$ ratios of reservoir fluids applying the three models for reconstruction of reservoir fluids from data on well fluid discharge (see text). The reservoir sulfide ratios of the fluids are very similar to those observed in basaltic rocks in Iceland (Sakai et al., 1980; Torssander, 1989) suggesting the same source of sulfide sulfur as in basalt either by magma degassing or basalt dissolution. Reservoir fluid sulfate ratios are heavier compared to sulfide ratios.

developed that takes into account possible sources and reactions of sulfur and sulfur isotopes upon progressive dissolution of primary rocks and formation of secondary minerals including sulfides. In the model, meteoric water was allowed to react with basalt in steps and the saturated secondary minerals were allowed to precipitate. The basalt was modeled as basaltic glass undergoing congruent dissolution and oxides were titrated into the rock in their relative molal abundance. The basaltic glass was assumed to contain 350 ppm S taken to be in the oxidation state $\text{S}^{-\text{II}}$ (Gunnlaugsson, 1977), and the concentrations of all other elements in the basaltic glass, as well as the compositions of the starting solution and the secondary minerals incorporated in the calculations were taken from Kaasalainen and Stefánsson (2012). This part of the modelling consisted of a conventional reaction path model and was conducted with the aid of the PHREEQC program (Parkhurst and Appelo, 1999). An overall redox equilibrium within the system was assumed; however, it should be pointed out that this assumption may not always be valid in geothermal systems

up to temperatures of $\sim 300^\circ\text{C}$ (Stefánsson and Arnórsson, 2002). From the reaction path calculation, the mole distribution of dissolved sulfide and sulfate species was obtained as well as the mass of secondary minerals formed as a function of reaction progress (ξ). The sulfur species observed to be significant were $\text{H}_2\text{S}(\text{aq})$, $\text{HS}^-(\text{aq})$ and SO_4^{2-} and the only secondary sulfur bearing mineral predicted to form was pyrite. The mass fraction of sulfur species and sulfur bearing minerals formed was subsequently combined with the multiple sulfur isotope fractionation factors (Table 2) to calculate sulfur isotope distribution in a similar manner as previously described, using

$$\begin{aligned} \delta^x\text{S}^{\text{total}} = & X_{\text{H}_2\text{S}(\text{aq})} \delta^x\text{S}_{\text{H}_2\text{S}(\text{aq})} \\ & + X_{\text{HS}^-} ((^x\alpha_{\text{HS}^- - \text{H}_2\text{S}(\text{aq})} (1000 + \delta^x\text{S}_{\text{H}_2\text{S}(\text{aq})}) - 1000) \\ & + X_{\text{pyrite}} ((^x\alpha_{\text{pyrite} - \text{H}_2\text{S}(\text{aq})} (1000 + \delta^x\text{S}_{\text{H}_2\text{S}(\text{aq})}) - 1000) \end{aligned} \quad (10)$$

The total sulfur isotopic composition of the system ($\delta^x\text{S}^{\text{total}}$) was taken to be zero, and to remain constant with

progressive reaction. A useful proxy for fluid–rock interaction is the reaction progress ξ , which can be quantified by the molar quantity of basalt dissolved per mass unit of solution. Fig. 9 shows the mole fraction distribution of $\text{H}_2\text{S}(\text{aq})$, $\text{HS}^-(\text{aq})$ and pyrite and their sulfur isotope composition as a function of reaction progress (ξ). The results demonstrate that upon progressive fluid–rock interaction sulfur is leached out of the primary rocks in the form of sulfide under the reduced conditions typically observed under geothermal

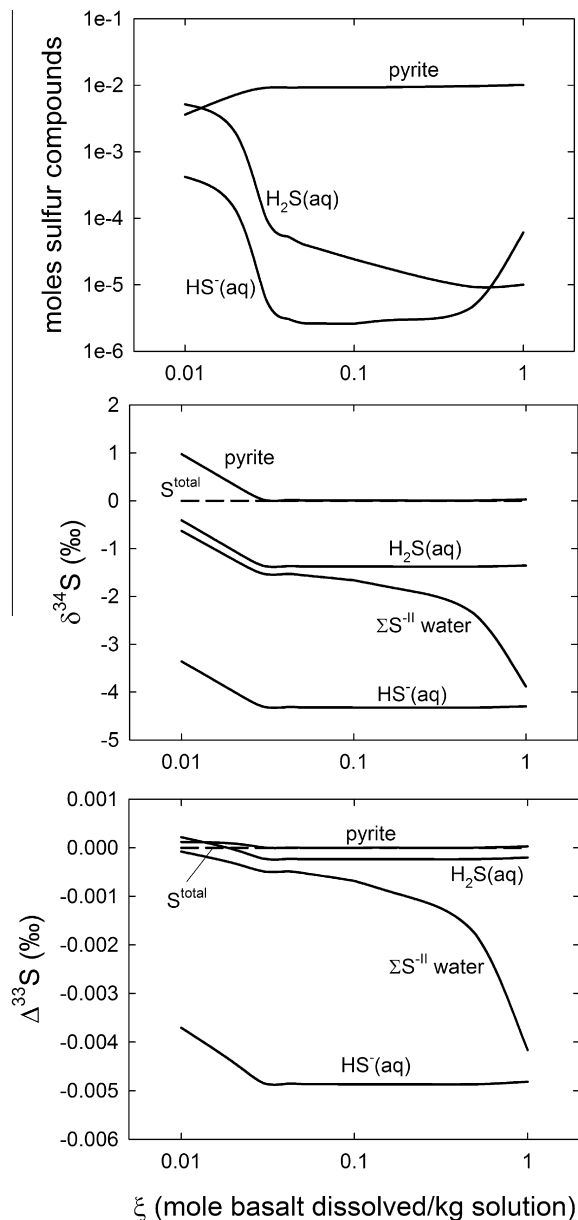


Fig. 9. The effect of progressive fluid–rock interaction on sulfur compound mole fractions and sulfur isotope values ($\delta^{34}\text{S}$ and $\Delta^{33}\text{S}$) of $\text{H}_2\text{S}(\text{aq})$, $\text{HS}^-(\text{aq})$ and total dissolved sulfide in the water phase, i.e. $\Sigma\text{S}^{\text{II}} = \text{H}_2\text{S}(\text{aq}) + \text{HS}^-$, and pyrite. The $\delta^{34}\text{S}$ and $\Delta^{33}\text{S}$ isotope values of the system were assumed to be zero. Upon progressive rock (basalt) dissolution (ξ) sulfide sulfur was leached from the rock, eventually leading to pyrite formation and an increase in pH. As a result, total dissolved sulfide in the liquid phase became isotopically lighter relative to pyrite.

conditions. This eventually leads to pyrite formation and sulfur isotope fractionation resulting in the fluids becoming progressively lighter relative to pyrite.

4.5. Source of sulfide in reservoir geothermal fluids

The effects of depressurization boiling and progressive fluid–rock interaction upon multiple sulfur isotope systematics in geothermal systems as at Krafla are shown in Fig. 10. As the fluid boiled upon ascent and progressive

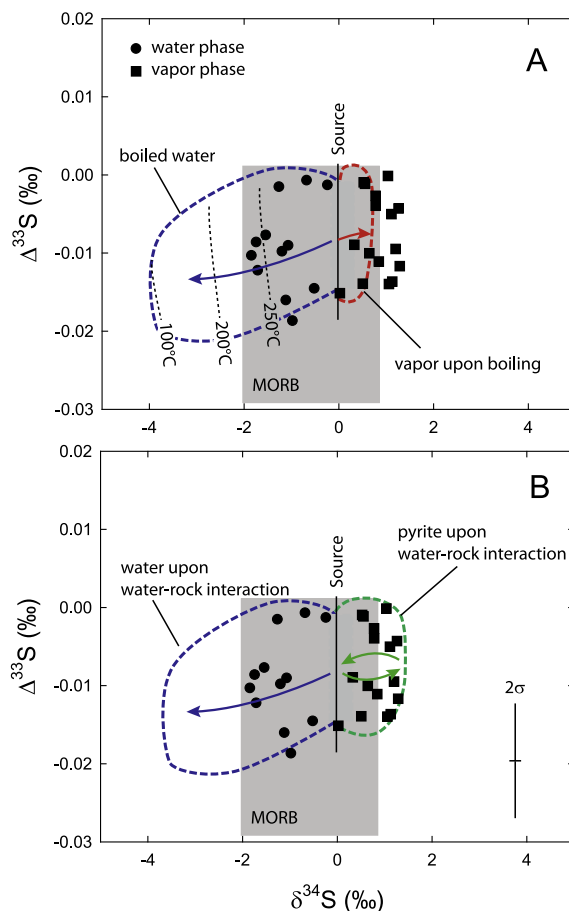


Fig. 10. Summary of the relationship between $\Delta^{33}\text{S}$ and $\delta^{34}\text{S}$ for sulfide in the water phase, vapor phase and pyrite upon depressurization boiling (A) and fluid–rock interaction (B). Shown are the sulfur isotope data for the liquid and vapor phases as sampled at the wellhead (circles and squares), as well as the results of the various models (blue, red and green dashed lines) for initial fluids of $\delta^{34}\text{S}$ equal to zero and $\Delta^{33}\text{S}$ in the range 0.00 to -0.015‰ . Upon depressurization boiling and progressive fluid–rock interaction the water phase became isotopically lighter relative to the source fluid with respect to $\delta^{34}\text{S}$ and $\Delta^{33}\text{S}$ ratios. In contrast, the vapor phase and pyrite became isotopically heavier with respect to $\delta^{34}\text{S}$ and $\Delta^{33}\text{S}$ ratios. This is indeed what was observed for two-phase well discharge fluids that had undergone boiling upon ascent to the surface. Also shown are the ranges of $\Delta^{33}\text{S}$ and $\delta^{34}\text{S}$ observed for Icelandic basalts and MORB (Sakai et al., 1980; Torssander, 1986, 1989; Labidi et al., 2012; Ono et al., 2012). The arrows show the isotopic trend with either progressive boiling or progressive water–rock interaction. (For interpretation of the references to colour in this figure legend, the reader is referred to the web version of this article.)

fluid–rock interaction with associated pyrite formation took place, the total sulfide (ΣS^{-II}) in the liquid phase progressively became isotopically lighter relative to the total system, both with respect to $\delta^{34}S$ and $\Delta^{33}S$. In contrast, the $H_2S(v)$ in the vapor phase and pyrite formed became isotopically heavier upon boiling and fluid–rock interaction, respectively. These results were in good agreement with the measured sulfur isotope ratios of sulfide in the vapor and liquid phases of the two-phase well discharges at Krafla, with $\delta^{34}S$ values of the vapor phase being heavier relative to $\delta^{34}S$ values of the liquid phase that were always negative. Similar observations were made for $\Delta^{33}S$ ratios, with the vapor phase being heavier relative to the water phase. The results of the modelling were also consistent with the $\delta^{34}S$ values for pyrite in Krafla reported by Sakai et al. (1980), covering a range from 0.0 to +0.9‰.

The conclusion drawn here is that the source of sulfide sulfur in the Krafla geothermal fluids is mid-ocean ridge basalt (MORB) with $\delta^{34}S$ values close to zero or in the range -2 to $+0.4$ ‰ (Sakai et al., 1980; Torssander, 1989; Labidi et al., 2012) and $\Delta^{33}S$ between 0.00 and -0.03 ‰ (Ono et al., 2012; Labidi et al., 2012). The variability in $\delta^{34}S$ and $\Delta^{33}S$ values of sulfide in the liquid and vapor phase are then caused by secondary processes, mainly boiling and progressive fluid–rock interaction, leading to an isotopically heavier vapor phase and isotopically lighter liquid phase. Distinguishing between the effects of boiling and fluid–rock interaction and sulfide mineralization on the multiple isotope systematics, however, is difficult.

4.6. Sulfate formation in high-temperature geothermal systems

In the Krafla geothermal system, sulfide is the dominant form of sulfur in the fluid at >230 °C accounting for >80 % of total sulfur on the molal basis in the reservoir fluids, the rest being mostly SO_4 . At temperatures <230 °C SO_4 becomes increasingly important, accounting for up to 55 mole% of total sulfur in the reservoir fluids.

The source of SO_4 in the geothermal fluids at Krafla is unclear. Possible sources include inorganic oxidation of sulfide, seawater sulfate input through meteoric water, or leaching from sulfate alteration minerals. The geothermal fluids at Krafla are dilute with reservoir Cl concentration between ~ 10 and ~ 150 ppm the exact concentration depending on the model applied for reconstruction of the reservoir fluid composition. Based on the low Cl concentrations together with major elemental chemistry and δD and $\delta^{18}O$ systematics it has been concluded that the Krafla geothermal fluids are of meteoric origin with negligible seawater recharge (Sveinbjörnsdóttir et al., 1986; Darling and Ármannsson, 1989; Pope et al., 2013). Dissolution of sulfate minerals is also considered unlikely as such minerals as anhydrite have not been identified in the altered rocks of the Krafla reservoir from the study of drill cuttings (Steinþórsson and Sveinbjörnsdóttir, 1981). This means that the most likely source of SO_4 in the geothermal fluids at Krafla is oxidation of H_2S to form SO_4 .

Many of the important processes contributing to the formation of sulfate may be visualized looking at the relationships between $\delta^{34}S$ for sulfate and sulfide including the temperature of the geothermal activity, if equilibrium fractionation has been received between sulfide and sulfate and about the source or ratio of H_2S to SO_4 in the system (Fifarek and Rye, 2005; Rye, 2005). An overall chemical equilibrium between H_2S and SO_4 (reaction 6) may not have been reached for the geothermal fluids at Krafla (Fig. 4). The same was true for the isotope equilibrium between ΣS^{-II} and SO_4 , with the ratio of $\delta^{34}S$ of ΣS^{-II} and SO_4 in the fluids corresponding to temperatures of ~ 320 to >700 °C, whereas the reservoir temperatures at Krafla were much lower or between ~ 200 and 450 °C (Fig. 11). Moreover, the ratio of ΣS^{-II} to SO_4 in the geothermal fluids falls close to a horizontal trendline suggesting that ΣS^{-II} is the only oxidation state of sulfur initially present in the geothermal system with a $\delta^{34}S$ value of -0.7 to -0.2 ‰ (Rye, 2005). Thus, the most likely source for SO_4 was oxidation of H_2S rather than SO_4 , even though equilibrium was not observed.

In Fig. 11 the time to reach sulfur isotope equilibrium between sulfate and sulfide is compared with the age of the geothermal fluids in Iceland based on tritium, C-14 and Ra isotopes systematics (Stefánsson et al., 2005;

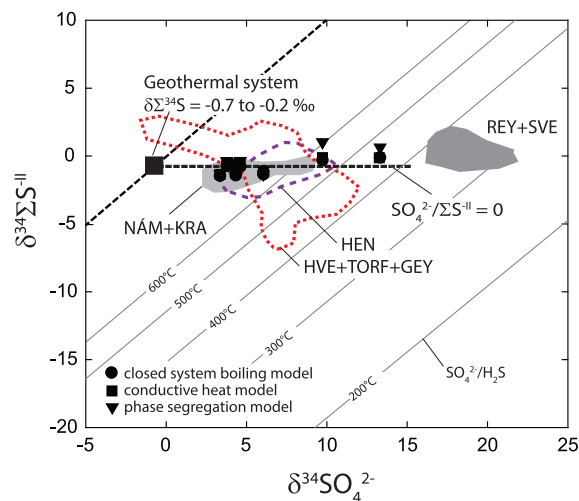


Fig. 11. Plot of $\delta^{34}S$ of sulfide versus sulfate for geothermal fluids in Iceland. The results of the three models used for calculation of the reservoir fluid composition based on fluid well discharge at surface are shown by the different symbols (circles, squares and triangles). Also shown are the ratios in geothermal fluids of various systems in Iceland previously published including Námafjall and Krafla (NÁM+KRA), Hengill (HEN), Hveravellir, Geysir and Torfajökull (HVE+TORF+GEY) and Reykjanes and Svartsengi (REY+SVE) (Torssander, 1986). The horizontal trend line observed for $\delta^{34}S$ of sulfide versus sulfate at Krafla suggests that the H_2S is the only form present in the geothermal system with an original $\delta^{34}S$ value between -0.7 and -0.2 ‰. The isotope ratios corresponded to temperatures of ~ 320 to >700 °C whereas the reservoir temperatures at Krafla were much lower or between ~ 200 to 450 °C, suggesting sulfur isotope disequilibrium between sulfide versus sulfate.

Kadko et al., 2007). The time to reach sulfur isotope equilibrium was calculated using the rate expression given by Ohmoto and Lasaga (1982):

$$\ln \frac{\alpha_e - \alpha_t}{\alpha_e - \alpha_0} = -kt \left(\sum S^{+VI} + \sum S^{-II} \right) \quad (11)$$

where k is the rate constant taken to be $k = \exp(-6.46 \cdot 10^3/T + 10.12)$ (in units of kg H₂O/mol·hr), α_0 is the initial fractionation factor of the system calculated from $\delta^{34}\text{S}$ for sulfide and sulfate in undegassed basalt (Torssander, 1986, 1989), α_t is the fractionation factor at time t calculated from the $\delta^{34}\text{S}$ values for sulfide and sulfate in the reservoir water, α_e is the fractionation factor at equilibrium taken to be $0.9 \alpha_0$ corresponding to 90% of the time needed to reach isotope equilibrium and $\sum S^{+VI} + \sum S^{-II}$ was taken as the total concentration of sulfur in the reservoir water. The times to reach sulfur isotope equilibrium between sulfide and sulfate in the reservoir fluids at Krafla were generally between ~1 and 35 years or on the same order of magnitude as the measured age of high-temperature Icelandic geothermal fluids (Stefánsson et al., 2005; Kadko et al., 2007). This suggests that the geothermal fluid residence times may be long enough to reach sulfur isotope exchange equilibria and thus contradicting the observations of sulfur isotope and chemical disequilibrium (Fig. 4 and 10).

The formation of SO₄ may be further explored through the relationship between $\Delta^{33}\text{S}$ and $\delta^{34}\text{S}$ for $\sum S^{-II}$ and SO₄ in the fluid. For this it was assumed that all sulfur in the fluid originated from basalt and entered the geothermal fluids, either upon magma degassing or basalt dissolution. Secondly, it was assumed that aqueous SO₄ was produced upon inorganic H₂S oxidation. During closed system H₂S oxidation in a single liquid system, the sulfur isotope ratios of the produced sulfate are expressed by (Ono et al., 2012):

$$\delta^x \text{S}_{\text{SO}_4} = (\delta^x \text{S}_{\text{H}_2\text{S}} + 1) \frac{1 - f^{\alpha_x}}{1 - f} - 1 \quad (12)$$

where $x = 33, 34$ and 36 , f the mol fraction of H₂S oxidized to SO₄ relative to initial H₂S and α the fractionation factor between SO₄ and H₂S. In the model we further assumed insignificant formation of sulfide minerals (e.g., Ohmoto and Goldhaber, 1997). Eq. (12) was solved for $\delta^x \text{SO}_4$ as a function of f for both ³³S and ³⁴S. For these calculations we assumed dissolved sulfide to be present as H₂S(aq); almost identical results would have been obtained using the HS⁻ to SO₄²⁻ fractionation factors. The starting $\delta^{34}\text{S}$ and $\Delta^{33}\text{S}$ were taken to be zero, within or close to the Icelandic basalts and MORB ratios previously reported (Sakai et al., 1980; Torssander, 1986, 1989; Labidi et al., 2012; Ono et al., 2012).

Alternatively, the origin of sulfate may be solely related to the source water, i.e. meteoric water, and mixing between basalt and meteoric water. The sulfate in meteoric water in Iceland originates predominantly from seawater spray, i.e. it has the same isotopic composition as seawater (Gíslason et al., 1996; Gíslason and Torssander, 2006), with values of seawater taken to be $\delta^{34}\text{S} +21.0\text{‰}$ and $\Delta^{33}\text{S} 0.050\text{‰}$ (Rees et al., 1978; Ono et al., 2012; Tostevin

et al., 2014). The other end-member is assumed to be basalt with the same sulfur isotope systematics as described above. A simple mixing between basaltic sulfur and seawater sulfate is described by

$$\delta^x \text{S}^{\text{gf}} = X^{\text{mw}} \delta^x \text{S}^{\text{mw}} + (1 - X^{\text{mw}}) \delta^x \text{S}^{\text{BAS}} \quad (13)$$

where $x = 33, 34$ and 36 , the superscripts gf, mw and BAS denotes geothermal fluid, meteoric water and basalt, respectively, and X^{mw} is the meteoric water mole fraction. (see Fig. 12).

The results of the calculations of multiple sulfur isotope systematics upon H₂S oxidation to SO₄ (Eq. (12)) and mixing between basaltic sulfur and seawater sulfate (Eq. (13)) are compared with the measured values in Fig. 13. As observed, H₂S values in the reservoir fluids are identical to those observed in MORB, whereas SO₄ displayed a much more positive $\delta^{34}\text{S}$ range (+2.1 to +13.4‰) and more negative range in $\Delta^{33}\text{S}$ values (−0.004 to −0.036‰) compared to H₂S. Such trends may be explained by mass-dependent fractionation upon moderate H₂S oxidation to SO₄ ($f > 0.1$) at temperatures observed in the geothermal reservoir of 200–300 °C. Mixing between meteoric water with sulfate of seawater origin and sulfur originated from the basalts either through magma degassing or upon basalt dissolution would result in positive $\Delta^{33}\text{S}$ with increasing $\delta^{34}\text{S}$, a trend not observed in these fluids.

The observed $\Delta^{33}\text{S}$ and $\delta^{34}\text{S}$ systematics for geothermal fluids at Krafla suggest that the source of sulfide in the fluids is the basaltic magma, either through degassing or dissolution of unaltered basalts, and sulfate to be formed

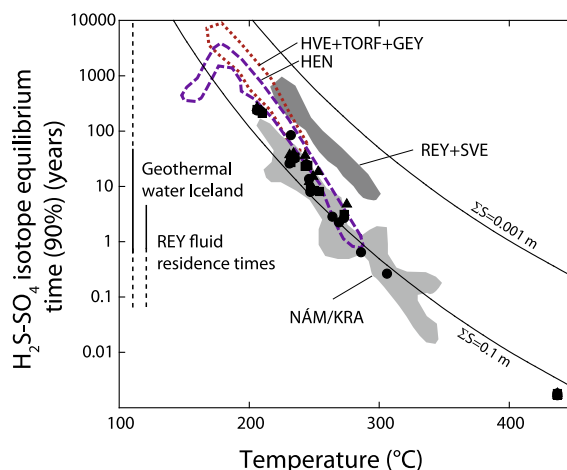


Fig. 12. The time it took to reach 90% of equilibrium isotope exchange between $\sum S^{-II}$ and SO₄ for Krafla reservoir fluids. Symbols are the same as in Fig. 11. The calculated equilibrium duration is generally between ~1 and ~35 years but may be as high as ~250 years for the fluids at <200 °C. The estimated residence time of geothermal fluids of various geothermal systems in Iceland is also shown for comparison, these being commonly between a year to a few decades in most cases but may be as long as >10,000 years (Stefánsson et al., 2005; Kadko et al., 2007). These findings suggest that the fluid residence times at Krafla and the times needed to reach sulfur isotope exchange equilibrium are most likely of the same magnitude.

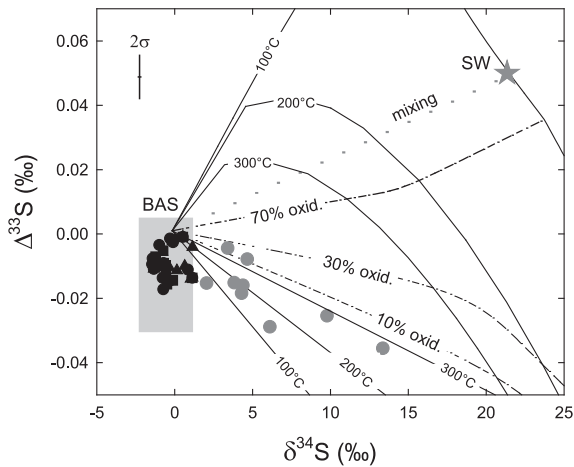


Fig. 13. The relationship between $\Delta^{33}\text{S}$ and $\delta^{34}\text{S}$ sulfide and sulfate in the reservoir fluids at Krafla. The results of the three models for reconstruction of reservoir fluids from data on well fluid discharge are shown. Black symbols represent reservoir sulfide (see Fig. 11), gray circles represent reservoir sulfate, SW denotes seawater and the gray shaded area is the range of sulfur isotope ratios for Icelandic basalts and MORB (Sakai et al., 1980; Torrsander, 1986, 1989; Labidi et al., 2012; Ono et al., 2012). Also shown is the mass dependent fraction between aqueous sulfide and sulfate according to the reaction $\text{H}_2\text{S}(\text{aq}) + 4\text{H}_2\text{O} = \text{SO}_4^{2-}(\text{aq}) + 2\text{H}^+ + 4\text{H}_2(\text{aq})$ at 100–300 °C and at various fractions (f) of H_2S oxidation (conversion) to SO_4 . Solid lines represent the $\Delta^{33}\text{S}$ and $\delta^{34}\text{S}$ values at a given temperature as a function of f (degree of oxidation) whereas the dashed lines represent a given degree of oxidation (10%, 30% and 70% oxidation) as a function of temperature. As observed, the heavy $\delta^{34}\text{S}$ and negative $\Delta^{33}\text{S}$ ratios of sulfate in the reservoir fluids may be explained by moderate oxidation of H_2S at similar temperatures as observed in the reservoir ($\sim 200\text{--}300$ °C) at Krafla. However, it should be kept in mind that neither chemical equilibrium nor sulfur isotope exchange equilibrium was observed between sulfide and sulfate in reservoir fluids (Figs. 5 and 11).

upon oxidation of the sulfide. Evidence in support of this includes: (1) the absence of sulfate minerals in the reservoirs of Krafla (Steinþorsson and Sveinbjörnsdóttir, 1981); (2) negligible contribution of seawater in the geothermal fluids at Krafla based on major elemental chemistry and δD and $\delta^{18}\text{O}$ systematics (Sveinbjörnsdóttir et al., 1986; Darling and Ármannsson, 1989; Pope et al., 2013); (3) decreasing $\Delta^{33}\text{S}$ with increasing $\delta^{34}\text{S}$ ratios of SO_4 from the source values of the system considered to be closely represented by MORB; (4) linear horizontal trend of $\delta^{34}\text{S}$ between $\Sigma\text{S}^{\text{II}}$ and SO_4 in the fluids (Rye, 2005). However, equilibrium between $\Sigma\text{S}^{\text{II}}$ and SO_4 was not observed (Fig. 4 and 11) despite the observation that fluid residence times in Icelandic high-temperature geothermal systems are similar to those needed to reach sulfur isotope equilibria between $\Sigma\text{S}^{\text{II}}$ and SO_4 (Ohmoto and Lasaga, 1982).

5. SUMMARY AND CONCLUSIONS

The multiple sulfur isotope systematics of the geothermal fluids at Krafla, Northeast Iceland, was studied in order to determine the source and reactions of sulfur in the system. Fluids from two-phase well discharges and

single phase vapor discharges were collected and analyzed for major elemental, sulfur speciation and multiple sulfur isotope composition. Based on these, the reservoir fluid composition was assessed using the open and closed system boiling model (Arnórrsson et al., 2007). The reservoir fluid temperatures ranged from 192 to 437 °C with liquid water and vapor being present in the reservoir. Dissolved sulfide ($\Sigma\text{S}^{\text{II}}$) and SO_4 predominated in the water phase with trace concentrations of S_2O_3 , whereas H_2S was the only sulfur species observed in the vapor phase. The $\delta^{34}\text{S}$ and $\Delta^{33}\text{S}$ values of sulfide in the reservoir liquid and vapor were between -1.5 and $+1.1$ ‰ and -0.017 and -0.001 ‰, respectively, whereas the $\delta^{34}\text{S}$ and $\Delta^{33}\text{S}$ of sulfate were significantly different or $+3.4$ to $+13.4$ ‰ and -0.036 ‰ to 0.000 ‰, respectively. Geochemical modelling was applied to investigate the effects of depressurization boiling and progressive fluid–rock interaction on the multiple sulfur isotope systematics. Depressurization boiling upon fluid ascent to the surface resulted in the liquid phase becoming progressively isotopically lighter, both with respect to $\delta^{34}\text{S}$ and $\Delta^{33}\text{S}$, whereas the H_2S in the vapor phase became isotopically heavier. This was in accordance with observed well discharge liquid and vapor sulfur isotope ratios. A similar trend occurred upon progressive fluid–rock interaction and pyrite formation, i.e. the liquid water became progressively isotopically lighter whereas the secondary pyrite became heavier. The observed $\Delta^{33}\text{S}$ and $\delta^{34}\text{S}$ systematics for geothermal fluids at Krafla suggest that the source of sulfides in the fluids is the basaltic magma, either through degassing or upon dissolution of unaltered basalts. The same is considered to be the source of SO_4 . At high temperatures, insignificant SO_4 concentrations were observed in the fluids whereas at lower temperatures significant concentrations of SO_4 were observed, the source considered to be oxidation of sulfide originating from basalt. The amount of sulfate originating from the meteoric source water of the geothermal fluids is considered to be negligible. Overall chemical and sulfur isotope equilibrium between $\Sigma\text{S}^{\text{II}}$ and SO_4 , however, was not observed. The findings of the present study indicate that the key sets of parameters influencing multiple sulfur isotope systematics of geothermal fluids under inorganic conditions are: (1) the isotopic composition of the source material or source fluid and (2) sulfur isotope fractionation associated with aqueous and vapor speciation related to progressive changes resulting from boiling, oxidation and fluid–rock interaction.

ACKNOWLEDGMENTS

This research was funded by the Geothermal Research Group (Project ID: 11-04-003) and Landsvirkjun Energy Research Fund. We would like to thank the associate editor, Jeffrey C. Alt and three anonymous reviewers for their detailed and constructive comments that led to substantial improvement of the manuscript.

REFERENCES

- Alt J. C. and Shanks W. C. (1998) Sulfur in serpentinized oceanic peridotites: Serpentinization processes and microbial sulfate reduction. *J. Geophys. Res.* **103**, 9917–9929.

- Arnórsson S., Gunnlaugsson E. and Svavarsson H. (1983a) The chemistry of geothermal waters in Iceland. II. Mineral equilibria and independent variables controlling water compositions. *Geochim. Cosmochim. Acta* **47**, 547–566.
- Arnórsson S., Gunnlaugsson E. and Svavarsson H. (1983b) The chemistry of geothermal waters in Iceland 2. Mineral equilibria and independent variables controlling water compositions. *Geochim. Cosmochim. Acta* **47**, 547–566.
- Arnórsson S., Bjarnason J. Ö., Giroud N., Gunnarsson I. and Stefánsson A. (2006) Sampling and analysis of geothermal fluids. *Geofluids* **6**, 203–216.
- Arnórsson S., Stefánsson A. and Bjarnason J. Ö. (2007) Fluid–fluid interactions in geothermal systems. *Rev. Min. Geochem.* **65**, 259–312.
- Bayon F. E. B. and Ferrer H. (2005) Sulphur isotope ratios in Philippine geothermal systems. In *Use of isotope techniques to trace the origin of acidic fluids in geothermal systems* (ed. F. D'Amore). IAEA, Austria, pp. 111–132.
- Bjarnason J. Ö. (2010) *The chemical speciation program WATCH, version 2.4*. ÍSOR – Iceland Geosurvey, Reykjavík, Iceland. Accessible at: <http://www.geothermal.is/software>.
- Coplen T. B. (2011) Guidelines and recommended terms for expression of stable-isotope-ratio and gas-ratio measurement results. *Rapid Commun. Mass Spectrom.* **25**, 2538–2560.
- Czarnacki M. and Halas S. (2012) Ab initio calculations of sulfur isotope fractionation factor for H₂S in aqua-gas system. *Chem. Geol.* **318–319**, 1–5.
- Darling W. G. and Ármannsson H. (1989) Stable isotope aspects of fluid flow in the Krafla, Námafjall and Theistdareykir geothermal systems of northeast Iceland. *Chem. Geol.* **76**, 197–213.
- Druschel G. K., Schoonen M. A. A., Nordstrom D. K., Ball J. W., Xu Y. and Cohn C. A. (2003) Sulfur geochemistry of hydrothermal waters in Yellowstone National Park, Wyoming, USA. III. An anion-exchange resin technique for sampling and preservation of sulfoxyanions in natural waters. *Geochem. Trans.* **4**, 12–19.
- Fifarek R. H. and Rye R. O. (2005) Stable-isotope geochemistry of the Pierina high-sulfidation Au–Ag deposit, Peru: influence of hydrodynamics on SO₄²⁻–H₂S sulfur isotopic exchange in magmatic-steam and steam-heated environments. *Chem. Geol.* **215**, 253–279.
- Giggenbach W. F. (1980) Geothermal gas equilibria. *Geochim. Cosmochim. Acta* **44**, 2021–2032.
- Giggenbach W. F. (1981) Geothermal mineral equilibria. *Geochim. Cosmochim. Acta* **45**, 393–410.
- Giggenbach W. F. (1992) Isotopic shifts in waters from geothermal and volcanic systems along convergent plate boundaries and their origin. *Earth. Planet. Sci. Lett.* **113**, 495–510.
- Giroud N. (2008) *A Chemical Study of Arsenic, Boron and Gases in High-Temperature Geothermal Fluids in Iceland*. Ph.D. thesis, University of Iceland.
- Gíslason S. R. and Torssander P. (2006) Response of sulfate concentration and isotope composition in Icelandic rivers to the decline in global atmospheric SO₂ emissions into the North Atlantic Region. *Environ. Sci. Technol.* **40**, 680–686.
- Gíslason S. R., Arnórsson S. and Ármannsson H. (1996) Chemical weathering of basalt in Southwest Iceland; Effects of runoff, age of rocks and vegetative/glacial cover. *Am. J. Sci.* **296**, 837–907.
- González-Partida E., Carrillo-Chávez A., Levresse G., Tello-Hinojosa E., Venegas-Salgado S., Ramirez-Silva G., Pal-Verma M., Tritilla J. and Camprubi A. (2005) Hydro-geochemical and isotopic fluid evolution of the Los Azufres geothermal field, Central Mexico. *Appl. Geochem.* **20**, 23–39.
- Gudmundsson B. Th. and Arnórsson S. (2005) Secondary mineral–fluid equilibria in the Krafla and Námafjall geothermal systems, Iceland. *Appl. Geochem.* **20**, 1607–1625.
- Gunnarsson I. and Arnórsson S. (2000) Amorphous silica solubility and the thermodynamic properties of H₄SiO₄ in the range of 0 to 350 °C at Psat. *Geochim. Cosmochim. Acta* **64**, 2295–2307.
- Gunnlaugsson E. (1977) *The origin and distribution of sulphur in fresh and geothermally altered rocks in Iceland*. Ph. D. thesis, University of Leeds, Leeds.
- Hayba D.O. and Ingebritsen S.E. (1994) The computer model HYDROTHERM, a three-dimensional finite-difference model to simulate ground-water flow and heat transport in the temperature range of 0 to 1200 °C: USGS Report 94–4045 85 pp.
- Henley R. W. and Hughes G. O. (2000) Underground fumaroles: “Excess heat” effects in vein formation. *Econ. Geol.* **95**, 453–466.
- Horne R. N., Satik C., Mahiya G., Li K., Ambusso W., Tovar R., Wang C. and Nassori H. (2000) *Steam–water relative permeability*. World Geothermal Congress, Kyushu-Tohoku, Japan.
- Johnson J. W., Oelkers E. H. and Helgeson H. C. (1992) Suprt92 – a software package for calculating the standard molal thermodynamic properties of minerals, gases, aqueous species, and reactions from 1 bar to 5000 bar and 0 °C to 1000 °C. *Comput. Geosci.* **18**, 899–947.
- Kaasalainen H. and Stefánsson A. (2011a) Chemical analysis of sulfur species in geothermal waters. *Talanta* **85**, 1897–1903.
- Kaasalainen H. and Stefánsson A. (2011b) Sulfur speciation in natural hydrothermal waters, Iceland. *Geochim. Cosmochim. Acta* **75**, 2777–2791.
- Kaasalainen H. and Stefánsson A. (2012) The chemistry of trace elements in surface geothermal waters and steam, Iceland. *Chem. Geol.* **330–331**, 60–85.
- Kadko D., Gronvold K. and Butterfield D. (2007) Application of radium isotopes to determine crustal residence times of hydrothermal fluids from two sites on the Reykjanes Peninsula, Iceland. *Geochim. Cosmochim. Acta* **71**, 6019–2029.
- Kamyshny A., Zilberbrand M., Ekeltchik I., Voitsekovski T., Gun J. and Lev O. (2008) Speciation of polysulfides and zerovalent sulfur in sulfide-rich water wells in Southern and Central Israel. *Aquat. Geochem.* **14**, 171–192.
- Labidi J., Cartigny P., Birck J. L., Assayg N. and Bourrand J. J. (2012) Determination of multiple sulfur isotopes in glasses: A reappraisal of the MORB δ³⁴S. *Chem. Geol.* **334**, 189–198.
- Li K. and Horne R. N. (2007) Systematic study of steam–water capillary pressure. *Geothermics* **36**, 558–574.
- Marini L., Moretti R. and Accornero M. (2011) Sulfur isotopes in magmatic-hydrothermal systems, melts, and magmas. *Rev. Min. Geochem.* **73**, 423–492.
- Matsuda K., Shimada K. and Kiyota Y. (2005) Isotope techniques for clarifying origin of SO₄ type acid geothermal-fluid. Case studies of geothermal areas in Kyushu, Japan. In: *Use of isotope techniques to trace the origin of acidic fluids in geothermal systems*. IAEA-TECDOC-1448, 83–95.
- Ohmoto H. and Rye R.O. (1979) Isotopes of sulfur and carbon. In: *Geochemistry of Hydrothermal Ore Deposits*. Barnes HL (ed.) J. Wiley and Sons, 509–567.
- Ohmoto H. and Lasaga A. C. (1982) Kinetics of reactions between aqueous sulfates and sulfides in hydrothermal systems. *Geochim. Cosmochim. Acta* **46**, 1727–1745.
- Ohmoto H. and Goldhaber M. B. (1997) Sulfur and carbon isotopes. In *Geochemistry of Hydrothermal Ore Deposits* (ed. H. L. Barnes). Wiley and Sons, pp. 517–611.
- Ono S., Wing B., Johnston D., Farquhar J. and Rumble D. (2006) Mass-dependent fractionation of quadruple stable sulfur isotope system as a new tracer of sulfur biochemical cycles. *Geochim. Cosmochim. Acta* **70**, 2238–2252.

- Ono S., Keller N. S., Rouxel O. and Alt J. C. (2012) Sulfur-33 constrains on the origin of secondary pyrite in altered oceanic basement. *Geochim. Cosmochim. Acta* **87**, 323–340.
- Otake T., Lasaga A. C. and Ohmoto H. (2008) Ab initio calculations for equilibrium fractionations in multiple sulfur isotope systems. *Chem. Geol.* **249**, 357–376.
- Parkhurst, D.L. and Appelo, C.A.J., (1999). User's guide to PHREEQC (Version 2) - A computer program for speciation, batch-reaction, one-dimensional transport, and inverse geochemical calculations. Report 99-4259, U.S. Geological Survey, Water-Resources Investigations.
- Pokrovski G. S. and Dubrovinsky L. S. (2011) The S³⁻ ion is stable in geological fluids at elevated temperatures and pressures. *Science* **331**, 1052–1054.
- Pope E. C., Bird D. K. and Arnórsson S. (2013) Evolution of low-¹⁸O Icelandic crust. *Earth Planet. Sci. Lett.* **374**, 47–59.
- Pritchett J. W. (2005) Dry-steam wellhead discharges from liquid-dominated geothermal reservoirs: A result of coupled nonequilibrium multiphase fluid and heat flow through fractured rock. In *Dynamics of Fluids and Transport in Fractured Rock* (eds. B. Faybishenko, P. A. Witherspoon and J. Gale). AGU, Washington, DC, pp. 175–181.
- Rees C. E., Jenkins W. J. and Monster J. (1978) The sulfur isotopic composition of ocean water sulfate. *Geochim. Cosmochim. Acta* **42**, 377–382.
- Robinson B.W. (1987) Sulphur and sulphate-oxygen isotopes in New Zealand geothermal systems and volcanic discharges; Studies on sulphur isotope variations in nature. Proceedings of an advisory group meeting, Vienna, 17–20 June 1985, IAEA, Vienna, pp. 31–48.
- Rye R. O. (2005) A review of the stable-isotope geochemistry of sulfate minerals in selected igneous environments and related hydrothermal systems. *Chem. Geol.* **215**, 5–36.
- Sakai H. (1983) Sulfur isotope exchange rate between sulfate and sulfide and its application. *Geothermics* **12**, 111–117.
- Sakai H., Gunnlaugsson E., Tómasson J. and Rouse J. E. (1980) Sulfur isotope systematics in Icelandic geothermal systems and influence of seawater circulation at Reykjanes. *Geochim. Cosmochim. Acta* **44**, 1223–1231.
- Scott S., Gunnarsson I., Arnórsson S. and Stefánsson A. (2014) Gas chemistry, boiling and phase segregation in a geothermal system, Hellisheidi, Iceland. *Geochim. Cosmochim. Acta* **124**, 170–189.
- Sorey M. L., Grant M. A. and Bradford E. (1980) Nonlinear effects in two-phase flow to wells in geothermal reservoirs. *Wat. Res. Res.* **16**, 767–777.
- Steinthórsson S. and Sveinbjörnsdóttir Á. E. (1981) Opaque minerals in geothermal well no. 7, Krafla, Northern Iceland. *J. Volcanol. Geotherm. Res.* **10**, 245–261.
- Stefánsson A. and Arnórsson S. (2002) Gas pressures and redox reactions in geothermal fluids in Iceland. *Chem. Geol.* **190**, 251–271.
- Stefánsson A., Arnórsson S. and Sveinbjörnsdóttir Á. E. (2005) Redox reactions and potentials in natural waters at disequilibrium. *Chem. Geol.* **221**, 289–311.
- Stefánsson A., Gunnarsson I. and Giroud N. (2007) New methods for the direct determination of dissolved inorganic, organic and total carbon in natural waters by Reagent-Free (TM) Ion Chromatography and inductively coupled plasma atomic emission spectrometry. *Anal. Chim. Acta* **582**, 69–74.
- Sveinbjörnsdóttir Á. E., Coleman M. L. and Yardley B. W. D. (1986) Origin and history of hydrothermal fluids of the Reykjanes and Krafla geothermal fields, Iceland. *Contrib. Min. Petrol.* **94**, 99–109.
- Thode H. G., Monster J. and Dunford H. B. (1961) Sulphur isotope geochemistry. *Geochim. Cosmochim. Acta* **25**, 159–174.
- Torssander P. (1986) *Origin of volcanic sulfur in Iceland – A sulfur isotope study*. Ph.D. thesis, Stockholm University, 164 pp.
- Torssander P. (1989) Sulfur isotope ratios of Icelandic rocks. *Contrib. Min. Petrol.* **102**, 18–23.
- Tostevin R., Turchynb A. V., Farquhar J., Johnstond D. T., Eldridgec D. L., Bishope J. K. B. and McIlvinf M. (2014) Multiple sulfur isotope constraints on the modern sulfur cycle. *Earth Planet. Sci. Lett.* **396**, 14–21.
- Xu Y., Schoonen M. A. A., Nordstrom D. K., Cunningham K. M. and Ball J. W. (1998) Sulfur geochemistry of hydrothermal waters in Yellowstone National Park: I. The origin of thiosulfate in hot spring waters. *Geochim. Cosmochim. Acta* **62**, 3729–3743.
- Xu Y., Schoonen M. A. A., Nordstrom D. K., Cunningham K. M. and Ball J. W. (2000) Sulfur geochemistry of hydrothermal waters in Yellowstone National Park, Wyoming, USA. II. Formation and decomposition of thiosulfate and polythionate in cinder pool. *J. Volcanol. Geotherm. Res.* **97**, 407–423.

Associate Editor: Jeffrey C. Alt